EVIDENCE FOR THE DECAY $\tau^+ \to \pi^+ \eta \bar{\nu}_\tau$

M. DERRICK, P. KOOIJMAN, J.S. LOOS [1], B. MUSGRAVE, L.E. PRICE, J. REPOND, K. SUGANO
Argonne National Laboratory, Argonne, IL 60439, USA

D. BLOCKUS, B. BRABSON, J.-M. BROM, C. JUNG, H. NEAL, H. OGREN, D.R. RUST
Indiana University, Bloomington, IN 47405, USA

C. AKERLOF, J. CHAPMAN, D. ERREDE, M.T. KEN, D. NITZ, R. THUN, R. TSCHIRHART
University of Michigan, Ann Arbor, MI 48109, USA

S. ABACHI, P. BARINGER, B.G. BYLSMA, R. DeBONTE, D. KOLTICK, F.J. LOEFFLER, E.H. LOW, R.L. McILWAIN, D.H. MILLER, C.R. NG, L.K. RANGAN [2], E.I. SHIBATA
Purdue University, West Lafayette, IN 47907, USA

and

B. CORK
Lawrence Berkeley Laboratory, Berkeley, CA 94720, USA

Received 12 February 1987

The inclusive production of η mesons in tau lepton decay has been studied using the High Resolution Spectrometer at the PEP e^+e^- facility. The data sample corresponds to an integrated luminosity of 300 pb^{-1} and the storage ring was operated at $\sqrt{s}=29$ GeV. The η production appears to be only compatible with the decay $\tau^+ \to \pi^+ \eta \bar{\nu}$, which violates isospin and G-parity conservation. The branching ratio of $5.1 \pm 1.5\%$ explains much of the current discrepancy between the one-prong topological branching ratio and the sum of the individual one-prong modes.

The measured properties of the tau lepton are in good agreement with its being the sequential lepton of the third quark–lepton generation [1] but, because of its high mass, it has many decay modes. Although τ decays to hadronic final states are dominated by the low-mass $J^P = 1^-$ and 0^-, 1^+ particles $\rho(770)$, π and $a_1(1270)$, the nature of the τ decays to higher multiplicity hadronic systems is not well understood [2]. The decay $\tau^+ \to \pi^+ \eta \bar{\nu}$ is of particular significance since the $(\pi^+ \eta)$ G parity is odd, but the J^P must be 0^+ or 1^-, so that, in the conventional picture, the decay violates *CVC* and occurs via a second-class vector current [3]. The decay mode $\tau^+ \to \pi^+ \eta \pi^0 \bar{\nu}$ is allowed and is expected to occur at a low level [2].

High-precision measurements [4] of the topological branching ratios to one, three and five charged particles have shown a significant discrepancy with the sum of the exclusive one-prong decays. The latter sum to $(78.7 \pm 2.1)\%$ whereas the one-prong topological branching ratio, B_1, is $(86.7 \pm 0.3)\%$. New measurements [5] of the rates for the leptonic modes $\tau \to \mu\nu\nu$ and $\tau \to e\nu\nu$ rule out a solution in which all one-prong exclusive modes are increased by a small amount to force agreement with B_1. The classification of the one-prong decays based on recent data [6] indicates a higher rate for the one-charged plus mul-

[1] Present address: Bell Laboratories, Naperville, IL 60566, USA.
[2] Present address: Lockheed Missiles and Space Co., Sunnyvale, CA 94086, USA.

tiple-neutral channel than was previously measured, suggesting that the solution lies with such decays. Since the η meson decays mainly to neutral channels, its production will contribute to resolving this discrepancy.

In this paper we report the first observation of η meson production in τ decay. The results are based on operation of the High Resolution Spectrometer [7] (HRS) at the PEP e^+e^- storage ring. The data used correspond to an integrated luminosity of 300 pb^{-1} and were taken at a center-of-mass energy of 29 GeV. The cuts used to select τ pair events have been described previously [8]. These data selections yielded 4004 events of the 1–1 topology and 2553 events of the 1–3 topology. The hadronic background is negligible for the 1–1 events and $5.2 \pm 1.0\%$ for the 1–3 topology.

The analysis depends on reconstructing $\eta \to \gamma\gamma$ decays via measurement of electromagnetic showers in the barrel shower counter [9]. Each of the 40 wedge-shaped modules consists of three sections: a $3X_0$ Pb-scintillator sandwich, a single-layer, 14-wire proportional chamber (PWC) in which the wires are aligned along the e^+e^- beam direction and finally an $8X_0$ Pb-scintillator sandwich. The PWC plane is at a radius of 2.03 m from the interaction point. Each of the two scintillator sections is read out by two phototubes, one at each end of the approximately 3 m long modules. The energy resolution is $(\sigma_E/E)^2 = 0.16^2/E + 0.06^2$, with E in GeV. The positions of the electromagnetic showers along the beam direction, z, are measured by current division in the PWC wires to an accuracy of ~ 2.5 cm.

Electromagnetic showers were defined using the following techniques established from e^+e^- annihilation data, test beam results, and Monte Carlo (MC) studies. The PWC wires whose pulse heights exceeded threshold were scanned in order to identify clusters of neighboring wires with similar z measurements. Clusters containing more than 11 wires were subdivided into two clusters at the wire with the smallest pulse height since the typical size of an electron/photon-induced cluster is less than eight wires. Next a match was sought between the charged track and the clusters. If the extrapolation of the track in the xy plane crossed the shower counter within three wires of the cluster and the projected z agreed with the average z measurement of the wires in the cluster, then that cluster was assigned to the charged track.

Clusters containing gaps of three or fewer wires were recombined into a single cluster unless

(a) both clusters were associated with charged particles or each contained large pulse heights;

(b) the total size of the recombined cluster was larger than 11 wires or the average z positions of the clusters were different outside of the measuring errors.

Finally, the energy as measured by the shower counter modules was distributed to the different clusters. If the module was hit by a charged particle but the analysis identified additional neutral clusters, the cluster associated with the charged particle was assigned the typical hadronic energy deposition of 200 MeV. The rest of the energy was distributed equally amongst the neutral clusters.

The background from spurious photons was minimized by requiring that any cluster in a one-prong hemisphere that was used for further analysis lie within a cone of 67° half angle relative to the direction of the charged particle. In addition, each event was required to have at least two clusters satisfying one or more of the two criteria: (I) the energy of each photon was larger than 100 MeV and neither photon shared the same shower counter module with other photons, or (II) the energy of each photon was larger than 1.0 GeV; in this case the photons were allowed to share the same shower counter module. Of the decay candidates that satisfy criterion I (II), 45% (75%) have two and only two clusters meeting these selections.

The distribution in effective mass ($M_{\gamma\gamma}$) was determined, after first reducing the combinatorial background involving γ rays from events with multiple π^0's. All γ clusters that contributed to a $\gamma\gamma$ mass in the range ($70\ \text{MeV} < M_{\gamma\gamma} < 210\ \text{MeV}$) with any other γ ray in the event were removed. In making this π^0 rejection, all neutral clusters with energy greater than 100 MeV were used, regardless of whether they shared a module with another γ ray. The $M_{\gamma\gamma}$ distribution obtained is shown in fig. 1. A clear η signal at 550 MeV is evident over an exponentially falling background.

The data have been fit to a Breit–Wigner (BW) contribution at the η mass, plus a background term consisting of a constant plus an exponential in $M_{\gamma\gamma}$. If the data are fit with the background term alone,

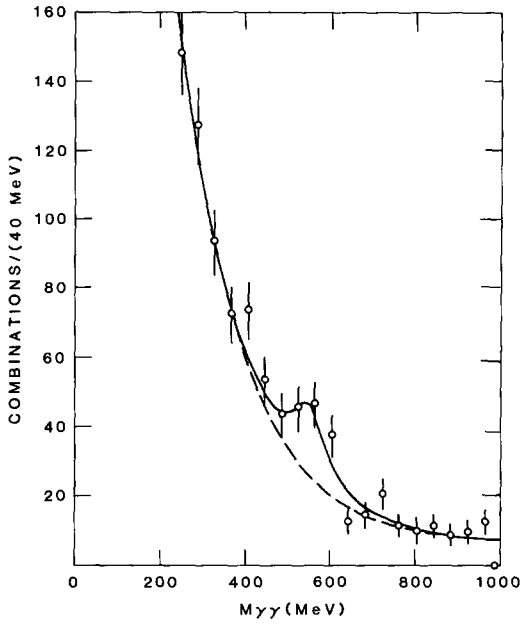

Fig. 1. Effective mass of $\gamma\gamma$ system for one-prong tau decays. All photons which, when combined with any other photon, yielded an $M_{\gamma\gamma}$ between 70 MeV and 210 MeV have been removed. Events satisfying both selection I and selection II are used but no combination is entered twice. The line shows the fit to the background function, consisting of an exponential in $M_{\gamma\gamma}$ and a constant term, plus a Breit–Wigner contribution to represent the η signal.

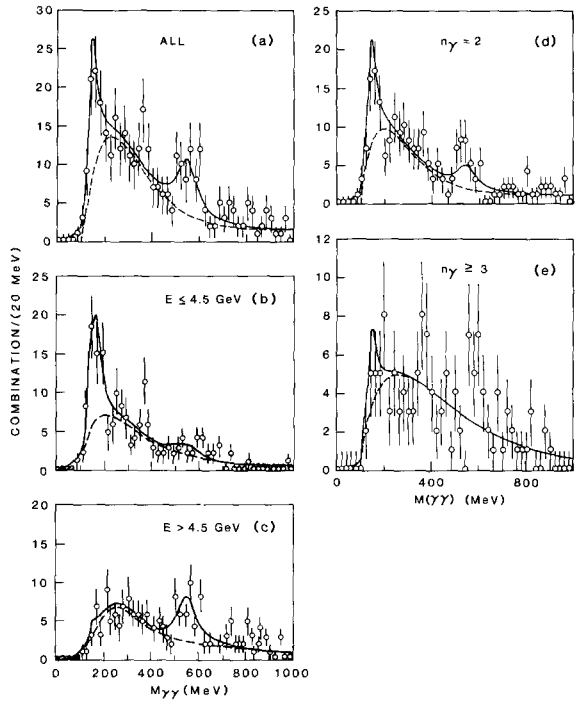

Fig. 2. Effective mass of $\gamma\gamma$ system for events with $E_{\gamma 1}$, $E_{\gamma 2} > 1$ GeV and having the photons in separate modules. (a) All combinations. (b) Combinations with $E_{\gamma 1}+E_{\gamma 2} \leq 4.5$ GeV. (c) Combinations with $E_{\gamma 1}+E_{\gamma 2} > 4.5$ GeV. (d) Events with two and only two photon clusters. (e) Events with three or more photon clusters. The lines show fits to the background function described in the text, plus contributions at the π^0 and η masses. In (e), the fit requires no η contribution.

the χ^2 is 26.7 for 17 degrees of freedom. The events in the η region contribute 10.9 to this χ^2, corresponding to a 3.3 standard deviation effect. If the FWHM of the BW is fixed at 100 MeV [‡1] and the fit is done including the η signal, a χ^2 of 17.3 is obtained for 16 degrees of freedom. The fit is shown by the solid line. In the η region (480 MeV $< M_{\gamma\gamma} <$ 620 MeV), there is a signal of 62 combinations over a background of 126.

We have also looked for events in which the η decays to $\pi^+\pi^-\pi^0$. The number of events observed is considered with those expected from the signal observed in the $\gamma\gamma$ decay mode.

Since the expected momentum spectrum of η mesons is hard and since photons from high-momentum π^0 decays almost always hit the same shower counter module, we show in fig. 2a the $\gamma\gamma$ mass spectrum for combinations where (i) the photons hit separate modules, (ii) $E_\gamma > 1$ GeV for both clusters, and (iii) no other photon shared the same module. A significant signal is seen both at the π^0 and at the η mass.

The data have been further divided into a low- and a high-energy sample with $E_{\gamma 1}+E_{\gamma 2}$ less than or greater than 4.5 GeV. As expected, the η signal persists in the $\gamma\gamma$ mass plot for the high-energy data of fig. 2c, but is less prominent in the low-energy spectrum of fig. 2b. The π^0 production populates the latter spectrum [‡2] primarily because of the requirement

[‡1] This value was taken from the Monte Carlo simulation of the η decay scaled down by 20%, a value obtained by comparing the observed and simulated width of the π^0 decay.

[‡2] There is also a peak at $M_{\gamma\gamma} \sim 380$ MeV in fig. 2b which has a statistical significance of 2.4 standard deviations. Since it is much narrower than the resolution, we ascribe this effect to a statistical fluctuation.

that the two photon clusters occur in separate modules: a module spans an azimuthal angle of 9°.

The events are distributed uniformly over the five years of data taking, and they do not preferentially populate any region of the detector. In addition, the signal does not depend on whether the recoiling τ decays to a one-prong or a three-prong topology. For the 1–1 topology, the track in the opposite hemisphere to that containing the η signal has the properties expected for normal τ decay. For the 1–3 topology, the mass distribution on the three-prong side of the charged particles plus all photons, is less than the τ mass within resolution. At most, two of the charged particles that accompany the η's have energy deposition consistent with that of an electron and the number of positively- and negatively-charged particles are equal within errors.

To study whether the one-prong τ-decay events come from the $\pi^+\eta\bar{\nu}$ or $\pi^+\eta\pi^0\bar{\nu}$ final states, the data of fig. 2a were subdivided into 229 events with two and only two neutral clusters (fig. 2d), and 145 $\gamma\gamma$ combinations from 113 events with three or more neutral clusters (fig. 2e). A minimum energy cut of 100 MeV was applied in defining a separate cluster. The enhancement at the η mass in the inclusive data persists in the events with only two photons, whereas there is no significant signal for $n_\gamma \geq 3$ selection. Photons from the $\pi^+\eta\pi^0\bar{\nu}$ final state can be missed either because they hit the cracks between modules or because they are coalesced with other photons in the event. Monte Carlo and other studies indicate that such effects are small – at about the 7% level. The 2γ data of fig. 2d is therefore clear evidence that the $\pi^+\eta\bar{\nu}$ final state is being observed.

The best fit lines in fig. 2, which represent the data well, have contributions at the π^0 and η masses, plus a background of the form

$$F(M_{\gamma\gamma}) = A + B(M_{\gamma\gamma} - M_{\gamma\gamma}^{\mathrm{th}})^{\alpha} \exp(-\beta M_{\gamma\gamma}),$$

where $M_{\gamma\gamma}^{\mathrm{th}}$ is a threshold mass taken as 100 MeV and A, B, α and β are free parameters. In the fit the area under the curve is normalized to the total number of events. The data of fig. 2e are well represented by the background term, plus a very small contribution for the π^0. The best fit requires no contribution at the η mass. The number of signal events in the η mass region, 480 MeV $< M_{\gamma\gamma} <$ 620 MeV, as compared to the background lines in fig. 2a, fig. 2d and fig. 2e, are listed in table 1.

Using a MC with full detector simulation, we studied the contributions of various final states to the backgrounds of fig. 2. The main contribution comes from the $\pi^+ 2\pi^0\bar{\nu}$ final state when the two photons from a π^0 decay are not resolved by the shower counter, but there is also a significant effect coming from misidentified photons from the $\pi^+\pi^0\bar{\nu}$ final state, since the branching ratio is large. For example, an interacting pion or a photon from initial state radiation can be mistaken for a photon from a final state decay in calculating the $\gamma\gamma$ effective mass. The events in fig. 2e with $n_\gamma \geq 3$ come predominantly from these background processes, but there is also a smaller contribution from the $\tau^+ \to \pi^+ 3\pi^0\bar{\nu}$ decay. These backgrounds are smooth in the η mass region.

Fig. 3 shows the $\gamma\gamma$ mass spectra with equivalent cuts to those used for the data of fig. 2 but applied to events resulting from an MC simulation of the decays $\tau^+ \to \pi^+\eta\bar{\nu}$ (figs. 3a–3c) and $\tau^+ \to \pi^+\eta\pi^0\bar{\nu}$ (figs. 3d–3f). The two neutral decay modes, $\eta \to \gamma\gamma$ and $\eta \to 3\pi^0$ were allowed with the known branching ratios. The MC simulation corresponds to about eight times the number of $\tau \to \eta$ events observed in the data. There is no π^0 peak in fig. 3 since the $\eta \to 3\pi^0$ decay usually gives a π^0 with energy below the 2 GeV cut.

As expected, the MC simulation of the $\pi^+\eta\bar{\nu}$ final

Table 1
Tau decay branching ratios.

γ selection	Figure	Events above background	Branching ratios for assumed final states	
			$\pi^+\eta\bar{\nu}$	$\pi^+\eta\pi^0\bar{\nu}$
all	2a	39 ± 8	$4.9 \pm 1.0\%$	$> 35\%$ at 90% CL
$n_\gamma = 2$	2d	26 ± 6	$5.3 \pm 1.3\%$	$> 11\%$ at 90% CL
$n_\gamma \geq 3$	2e	10 ± 5	–	$16 \pm 8\%$

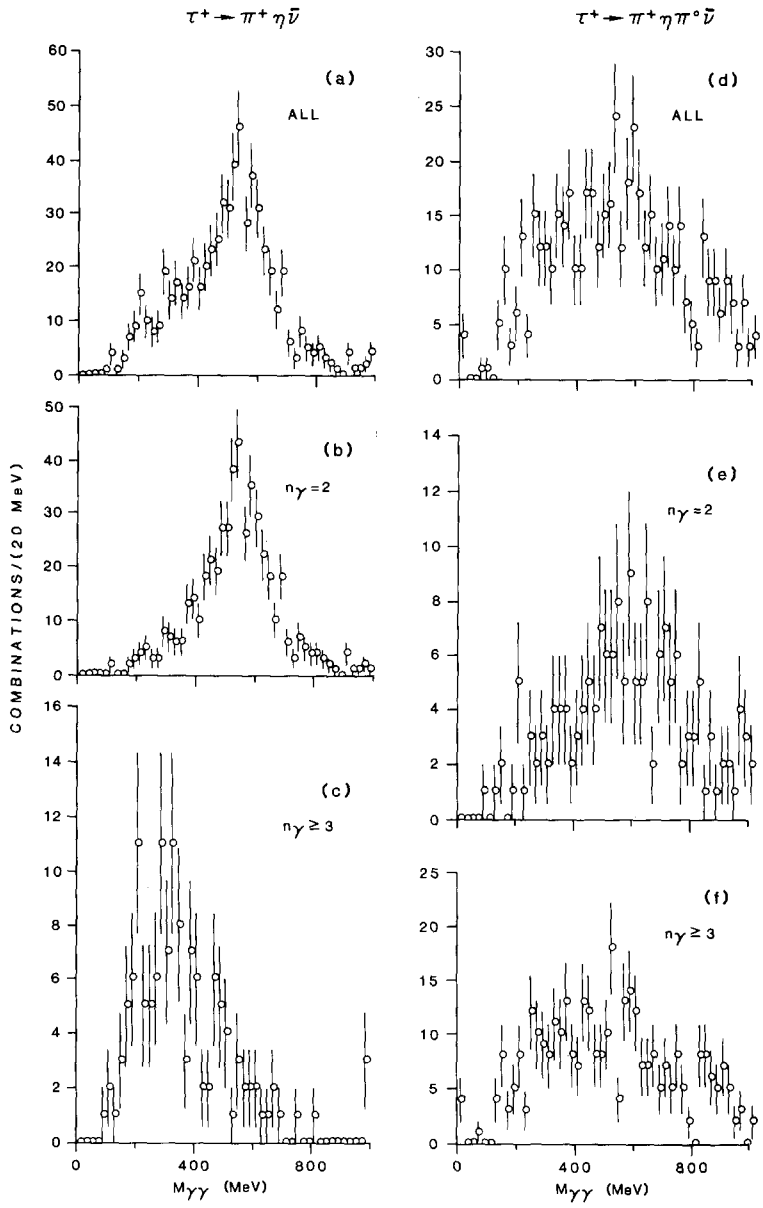

Fig. 3. Effective mass distributions for $\gamma\gamma$ combinations from $\eta \to \gamma\gamma$ and $\eta \to 3\pi^0 \to 6\gamma$ decays according to the Monte Carlo simulation (a) $\tau^+ \to \pi^+ \eta \bar{\nu}$ decay, all events; (b) $\tau^+ \to \pi^+ \eta \bar{\nu}$ decay, events with two and only two photon clusters; (c) $\tau^+ \to \pi^+ \eta \bar{\nu}$ decay, events with three or more photon clusters; (d) $\tau^+ \to \pi^+ \eta \pi^0 \bar{\nu}$ decay, all events; (e) $\tau^+ \to \pi^+ \eta \pi^0 \bar{\nu}$ decay, events with two and only two photon clusters;(f) $\tau^+ \to \pi^+ \eta \pi^0 \bar{\nu}$ decay, events with three or more photon clusters.

state shows a strong enhancement in the $\gamma\gamma$ mass spectrum near 550 MeV in fig. 3a and fig. 3b. The shoulder at lower masses comes from $\gamma\gamma$ combinations with photons from separate π^0's from the $\eta \to 3\pi^0$ decay. Only a small fraction of the events satisfy the selection $n_\gamma \geq 3$ and, as seen in fig. 3c, there is no η signal in these events.

The MC simulation of the $\pi^+ \eta \pi^0 \bar{\nu}$ final state, shown in figs. 3d–3f, has a poor signal to noise ratio at the η peak because of the combinatorial back-

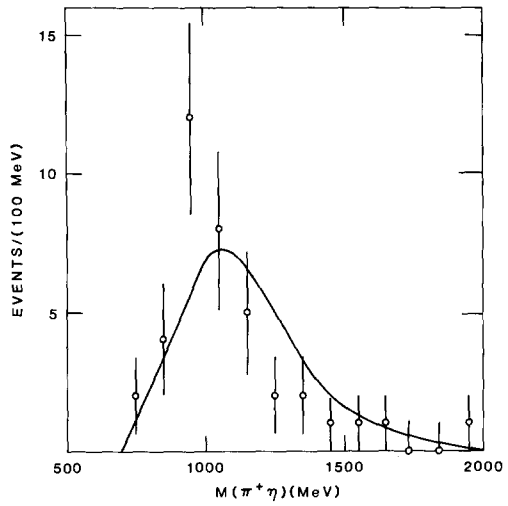

Fig. 4. Effective mass distribution of $\pi^+\eta$. The line shows the results of a Monte Carlo simulation of the $\tau^+ \to \pi^+ \eta\bar{\nu}$ decay, according to phase space and including the detector acceptance.

ground with one photon from the η decay combining with one from the π^0. For this final state, only one-third of the events satisfy the $n_\gamma = 2$ selection; most of the $\eta \to 2\gamma$ decay events are found in fig. 3f which has $n_\gamma \geq 3$. However, even with this cut, the η peak is not prominent.

The comparison of the data of fig. 2 with the MC simulations of the $\pi^+\eta\bar{\nu}$ and $\pi^+\eta\pi^0\bar{\nu}$ final states, shown in fig. 3, clearly indicates that most of the signal results from the decay $\tau^+ \to \pi^+ \eta\bar{\nu}$. This point is quantified in the decay branching ratios given in table 1. They are calculated assuming that the final state is either $\pi^+\eta\bar{\nu}$ or $\pi^+\eta\pi^0\bar{\nu}$ and use the event numbers given in table 1 and the acceptance estimated from the MC simulation for these final states. The two values for the $\pi^+\eta\bar{\nu}$ final state are consistent within errors, whereas the $\pi^+\eta\pi^0\bar{\nu}$ hypothesis gives unreasonably large decay branching ratios for all of the data selections of fig. 2.

The best value for the branching ratio for $\tau^+ \to \pi^+ \eta\bar{\nu}$ is $(5.1 \pm 1.0 \pm 1.2)\%$ [13]. The systematic uncertainty is estimated from the uncertainty in the acceptance calculation, from the results of a separate analysis that uses a different algorithm for identifying the photon clusters and from the unknown branching ratio for the $\pi^+\eta\pi^0\bar{\nu}$ final state.

The question arises whether the decay $\tau^+ \to \pi^+ \eta\bar{\nu}$ occurs through the intermediate $a_0(980)$ scalar meson: $\tau^+ \to a_0^+(980)\bar{\nu} \to \pi^+\eta\bar{\nu}$. Fig. 4 shows the $\pi^+\eta$ mass spectrum for the η events of fig. 2d, which have a signal-to-background ratio of two to one. The photon clusters were kinematically constrained to the $\eta \to \gamma\gamma$ decay hypothesis. The line, which is normalized to the data, shows the result of the MC simulation of the $\tau^+ \to \pi^+ \eta\bar{\nu}$ decay, according to phase space, and including the experimental selections. It also peaks near 1 GeV, but is somewhat wider than the data. The decay angular distribution relative to the line of flight of the $\pi^+\eta$ system is consistent with being isotropic. We conclude that, with the present number of events, although the data are consistent withan $a_0(980)$ intermediate state, we are unable to establish this decay mode.

The present results show evidence for a second-class current contribution to τ decay. There is, of course, the possibility that final state interactions produce an unexpectedly large isospin violation in the $\tau^+ \to \pi^+ \eta\bar{\nu}$ decay channel. The results are not in disagreement with searches for second-class current, in nuclear β decay, in muon capture, and in neutrino interactions [11]. Theoretical estimates [12] based on an assumed maximal second-class current contribution to the $\tau^+ \to \pi^+ \eta\bar{\nu}$ decay give branching ratios of (4–6)% in agreement with our measurement.

In this letter, we report the observation of η production in one-prong τ decays and give evidence for the decay $\tau^+ \to \pi^+ \eta\bar{\nu}$. The branching ratio of 5.1% gives a 3.6% contribution to the one-prong topology since the branching ratio of η to neutrals is 71%. This result goes far in accounting for the one-prong deficit. The discrimination between the $\pi^+\eta\bar{\nu}$ and $\pi^+\eta\pi^0\bar{\nu}$ final states rests on (i) the absence of additional photons in the events in which the $\eta \to \gamma\gamma$ decay is detected, (ii) the overall consistency of the data with characteristics expected from the $\tau^+ \to \pi^+ \eta\bar{\nu}$ decay, and (iii) the difference of the data from the simulation of the $\tau^+ \to \pi^+ \eta\pi^0\bar{\nu}$ decay leading to a low detection efficiency and a correspondingly large and unreasonable branching ratio.

Second-class current are not included in the known parts of the standard model of electroweak interactions, so it is important that the results reported in

[13] In this experiment charged pions and kaons are not differentiated. However, the interpretation of the decay as $\tau^+ \to K^+ \eta\bar{\nu}$ is inconsistent with the known kaon production in τ decay (see ref. [10]).

this letter be confirmed or denied by other, independent experiments on τ decay.

We express our gratitude to the SLAC cryogenic group, to the technical staffs of PEP, and of the collaborating institutions, without whom this experiment would not have been possible. This work was supported in part by the US Department of Energy under Contracts W-31-109-ENG-38, DE-AC02-76ER01112, DE-AC03-76F00098, DE-AC02-76ER01428, and DE-AC02-84ER40125.

References

[1] M.L. Perl, Ann. Rev. Nucl. Part. Sci. 30 (1980) 299.
[2] F.J. Gilman and S.H. Rhie, Phys. Rev. D 31 (1985) 1066.
[3] S. Weinberg, Phys. Rev. 112 (1958) 1375.
[4] K.K. Gan, Proc. Oregon DPF Meeting, ed. R.C. Hwa (World Scientific, Singapore, 1985) p. 248.
[5] R.M. Baltrusaitis et al., Phys. Rev. Lett. 55 (1985) 1842; W.W. Ash et al., Phys. Rev. Lett. 55 (1985) 2118.
[6] H. Aihara et al., Phys. Rev. Lett. 57 (1986) 1836; P.R. Burchat et al., Phys. Rev. D 35 (1987) 27.
[7] D. Bender et al., Phys. Rev. D 30 (1984) 515; M. Derrick et al., Phys. Rev. D 34 (1986) 3286, 3304.
[8] K.K. Gan et al., Phys. Lett. B 153 (1985) 116; C. Akerlof et al., Phys. Rev. Lett. 55 (1985) 570.
[9] J.S. Loos et al., Nucl. Instrum. Methods A 249 (1986) 185.
[10] G.B. Mills et al., Phys. Rev. Lett. 52 (1984) 1944.
[11] L. Grenachs, Ann. Rev. Nucl. Part. Sci. 35 (1985) 455; B. Holstein, Phys. Rev. C 29 (1984) 623; S.J. Barish et al., Phys. Rev. D 16 (1977) 3101.
[12] C. Leroy and J. Pestieau, Phys. Lett. B 72 (1978) 398; S.N. Biswas et al., Phys. Lett. B 80 (1980) 393; N. Paver and D. Treleani, Lett. Nuovo Cimento 31 (1981) 364; V.P. Barannik, A.P. Korzh and M.P. Rekalo, Acta Phys. Pol. B 13 (1982) 835.